SINGLE BEAM INTERFEROMETRY OF A THERMAL BUMP: II--THEORY

L. D. Favro and M. Munidasa

Department of Physics
Wayne State University
Detroit, MI 48202

INTRODUCTION

Kuo and Munidasa [1] have reported a method by which a time-dependent optical intensity pattern is produced by the interference of laser light diffracted from a thermally induced bump with the light of the same laser reflected from the plane of the sample on which the bump was induced. In their experiment the thermal bump was induced by a second laser beam which was optically incoherent with the interfering light, but which was intensity modulated at frequencies ranging from the audio to the ultrasonic range. The resulting time-dependent patterns carry information about the thermal and elastic properties of the sample. The purpose of this work is to provide a first-principles calculation of those patterns so that those material properties can be measured with this technique. The starting point of the calculation is the solution to the coupled thermoelastic equations developed by Favro et al. [2-4]. That solution is expressed in terms of the three eigenmodes of the coupled equations: (1) a longitudinal acoustic wave consisting of propagating particle displacements and associated temperature variations arising from the compression and rarefaction of the material; (2) a transverse (shear) wave which consists only of propagating particle displacements and which does not cause any temperature variation as it propagates; and (3) a heavily-damped thermal wave which consists of propagating temperature variations and associated particle displacements arising from the thermal expansion it causes. The combination of surface displacements (i.e. "thermal bump") resulting from these three kinds of waves when a modulated laser beam is incident on the surface of an opaque solid can be calculated in a straight forward fashion from expressions given in [4]. If the heating beam is centered at the origin in the plane $z=0$, the result of these calculations is given by the formula,

$$h(x,y,t) = \int_0^\infty \Phi(p,t)\, J_0[p(x^2+y^2)^{1/2}]\, e^{-\frac{p^2R^2}{4}}\, p\, dp \quad , \tag{1}$$

or equivalently,

$$h(x,y,t) = \iint dp_x dp_y\, \Phi(p,t)\, e^{-\frac{p^2R^2}{4}}\, \frac{e^{i(p_x x + p_y y)}}{2\pi} \quad , \tag{1'}$$

where J_0 is the zero-order Bessel function,

$$\Phi(p,t) = -k_s^2 R_1 \frac{(p_1 - p_3)(2p^2 - k_s^2)\, e^{-i\omega_0 t}}{p_3[(2p^2 - k_s^2)^2 + 4p^2 p_1 p_2]} \quad , \tag{2}$$

$$R_1 = \frac{\alpha(3\lambda + 2\mu)}{(\lambda + 2\mu)(q^2 - k_0^2)} \quad , \tag{3}$$

and where ω_0 is the (angular) modulation frequency, R the (Gaussian) radius of the incident beam, α the thermal expansion coefficient, λ the Lamé constant, μ the shear modulus, q the thermal-wave wave number, k_s the shear wave number, and k_0 the longitudinal wave number. The integration variable p is effectively the radial component of all three waves' wave-vectors, and the quantities p_1,p_2, and p_3 are the normal components of those wave-vectors given by $(k_0^2 - p^2)^{1/2}$, $(k_s^2 - p^2)^{1/2}$, and $(q^2 - p^2)^{1/2}$ respectively. Although this result is written in a compact form as one term, it is actually the sum of four terms, each representing a different physical contribution to the bump. The terms which contribute consist of the normal components of the motion associated with, the directly generated longitudinal wave and its reflection from the surface, the longitudinal wave generated at the surface by mode conversion of the thermal wave, the shear wave generated at the surface by the mode conversion of the thermal wave, and the shear wave generated at the surface by mode conversion of the directly generated longitudinal wave. There is no normal displacement associated with the thermal waves themselves, because the normal displacements associated with the incident and reflected thermal waves are in opposite directions, and cancel each other to a high degree of precision.

When a probe laser beam is incident on the surface exhibiting the bump described by Eq.(1), the reflected and diffracted beam can be calculated by assuming the surface struck by the beam to be a source of secondary wavelets (Huygens principle). If the probe beam has a Gaussian profile and is incident in the normal (negative z) direction on the surface, the incident probe beam amplitude can be expressed as (see Ref. [1]),

$$E(x,y,z,t) = -iE_0 \frac{z_0}{(z_1 - z - iz_0)} e^{i[k(z_1 - z) - \omega t]} e^{ik \frac{[(x - x_0)^2 + (y - y_0)^2]}{2(z_1 - z - iz_0)}} \quad , \tag{4}$$

where the parameter z_0 determines the radius of the waist of the probe beam through the relation $w_0 = (2z_0/k)^{1/2}$, and where the waist is located at $z = z_1$. E_0 is the amplitude of the wave at the waist, ω is the optical frequency, and the beam is centered at the point (x_0,y_0) on the surface. With the surface of the sample taken to be at $z = 0$, the reflected wave given by Huygens principle can be written as,

$$E_r = \frac{-ik}{2\pi} \iint dx'\, dy' \left[\frac{e^{ik|\mathbf{r} - \mathbf{r}'|}}{|\mathbf{r} - \mathbf{r}'|} E(x',y',z',t) \right]_{z' = h(x',y',t)} \quad . \tag{5}$$

It should be noted here that the time dependences in Eqs. (1) and (4), although written as complex numbers, are implicitly real. Therefore care must be taken in combining them in Eq. (5) to ensure that the two real parts are taken separately and no mixing of the complex numbers occurs.

In the Kuo-Munidasa experiment, the observation distances are such that the diffraction pattern from the thermal bump is in the Fresnel regime. Therefore the phase in the exponential factor in Eq. (5) must be accurate at least to second order in the variables x' and y'. However, since the bump height is of the order of an Ångstrom or less, the dependence on z' need only be retained to first order. In fact, z' (=h(x',y',t)) is so small that the approximation,

$$e^{ikz'} \cong 1 - ikh(x',y',t) \tag{6}$$

is always valid. Hence, the reflected probe beam will consist of two terms. The first is the contribution of the "1" in Eq. (6) which corresponds to zero bump height. This term just produces a reflection of the Gaussian probe beam from the surface z=0. The second is the contribution of the second term in Eq. (6). This term produces a diffraction pattern of the thermal bump. It is the interference of this diffracted beam with the reflected beam produced by the first term which is responsible for the interference pattern in the experiment. The pattern is effectively a hologram of the bump, with the rôle of the reference beam's being played by the first term in Eq. (6). With the approximations described above in mind, we may write the reflected probe beam as,

$$E_r \cong \frac{-ik}{2\pi}\iint dx'\,dy' \frac{e^{ikz}}{z}\, e^{ik\frac{[(x-x')^2+(y-y')^2]}{2z}} E(x',y',0,t)\,[1 - 2ikh(x',y',t)] \quad . \tag{7}$$

It should be noted here that there are two contributions (and hence a factor of 2) from the height of the bump in this expression. The first comes from the (-ikz) term in the first exponential in Eq. (4). It represents the phase shift that results from the fact that the incident beam strikes the bump sooner than it strikes the surrounding surface. The second, which represents the corresponding phase shift in the outgoing wave, comes from the exponential in Eq. (5). If the expression (1') for the bump height is substituted into Eq. (7), the integrations over x' and y' can be performed analytically leaving only the p_x and p_y integrations to be performed. When this is done the result consists of two terms. One, with no remaining integrations, just represents the reflected probe beam, and is of the same form as Eq. (4) but with the sign of z changed. Its time dependence is entirely at the optical frequency ω. The other, the term arising from the bump, contains the remaining integrations and has the optical frequency mixed with the modulation frequency ω_0. When the sum of these two terms is squared, the cross terms beat at the modulation frequency and produce the time-dependent interference pattern. Since the total expression is rather cumbersome, we will present only these time-dependent interference terms here, and will compact the notation somewhat by replacing the variables (x,y) and the beam offset position (x_0,y_0) by the two-dimensional vectors $\mathbf{r}$ and $\mathbf{r}_0$ respectively. The interference term is then given by,

$$I = \frac{-k}{\pi} I_0 \iint dp_x dp_y\, \Phi(p,t)\, e^{-\frac{p^2R^2}{4}}\, [\mathrm{Im}]\left[e^{\frac{z(z_1 - iz_0)p^2}{2ik(z_1+z-iz_0)}}\, e^{i\frac{\mathbf{p}\cdot[z\mathbf{r}_0 + (z_1 - iz_0)\mathbf{r}]}{(z_1+z-iz_0)}} \right] , \tag{8}$$

where the symbol [Im] indicates the taking of the imaginary part of the expression in the brackets that follow, and where the multiplicative factor I_0 is the intensity of the reflected probe beam given by,

$$I_0 = \frac{E_0^2 z_0^2}{(z_1+z)^2 + z_0^2}\, e^{-\frac{kz_0(\mathbf{r}-\mathbf{r}_0)^2}{(z_1+z)^2+z_0^2}} \quad . \tag{9}$$

There is one special case in which one of the two remaining integrations In Eq. (8) can be performed analytically. This occurs when the vectors $\mathbf{r}$ and $\mathbf{r}_0$ are parallel, corresponding to the physical situation in which the point of observation is in the same vertical plane as the offset line between the heating and probe beams. If we take this line to be along the x-axis, Eq. (8) can be simplified to the form,

$$I = -2k I_0 \int_0^\infty p\,dp\, \Phi(p,t)\, e^{-\frac{p^2R^2}{4}}\, [\mathrm{Im}]\left\{ e^{\frac{z(z_1 - iz_0)p^2}{2ik(z_1+z-iz_0)}} J_0\left[\frac{zx_0 + (z_1 - iz_0)x}{(z_1+z-iz_0)}\right] \right\} \quad . \tag{10}$$

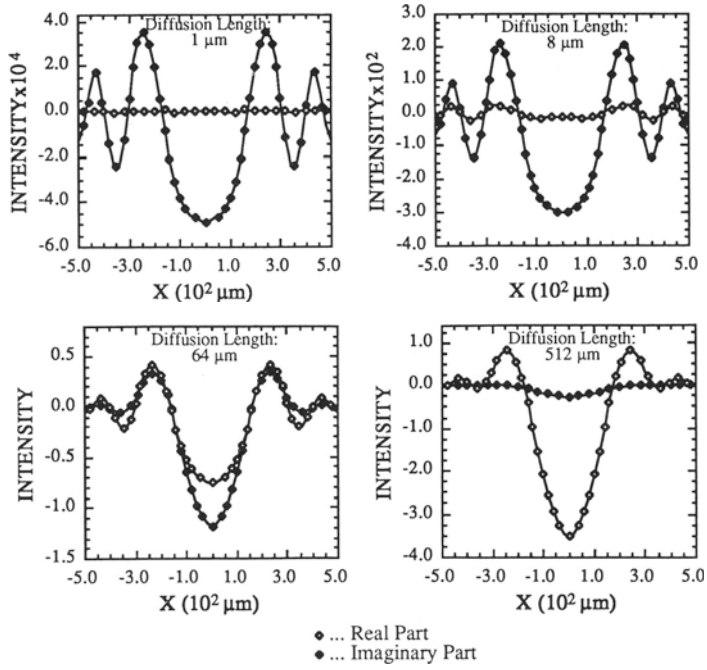

Fig. 1. Intensity distributions at a distance of 10 cm from the sample as a function of scan distance for 4 different values of the diffusion length. The vertical scale is arbitrary but the relative scales from plot to plot are correct.

Figure 1 shows typical ac diffraction patterns at a distance of 10 cm from the sample calculated from Eq. (10) for the case of a 20 μm diameter heating beam, with the offset between the heating and probe beams set equal to zero, and with thermal diffusion lengths of 1, 8, 64 and 512 μm. Each change in diffusion length corresponds to a (downward) change of the modulation frequency by a factor of 64. It should be noted that these changes have two obvious effects. One is the increase in the magnitude of the signal with decreasing frequency (increasing diffusion length). This results from the increased time for heating during the modulation period which produces both an increased bump height, and an increased lateral extent of the bump. This change in the bump configuration can be seen in Fig. 2, which shows the real and imaginary parts of the bump heights calculated from Eq. (1) for three different ratios of the diffusion length to the heating-beam radius. The other obvious effect of the changing frequency in the curves of Fig. 1 is the steady increase in the importance of the real part of the signal with respect to the imaginary part as the diffusion length increases. This is the result of the corresponding changes in phase which occur in the bump height as seen in Fig. 2. Figure 3 is similar to Fig. 1 except that the offset between the heating and probe beams is set equal to 200 μm. This causes the interference patterns to lose their left-right symmetry.

Equations (8) and (10), from which the results above were calculated, were derived under the assumption that the probe beam was normally incident on the surface of the sample. In the Kuo-Munidasa experiment the probe beam is usually tilted away from the

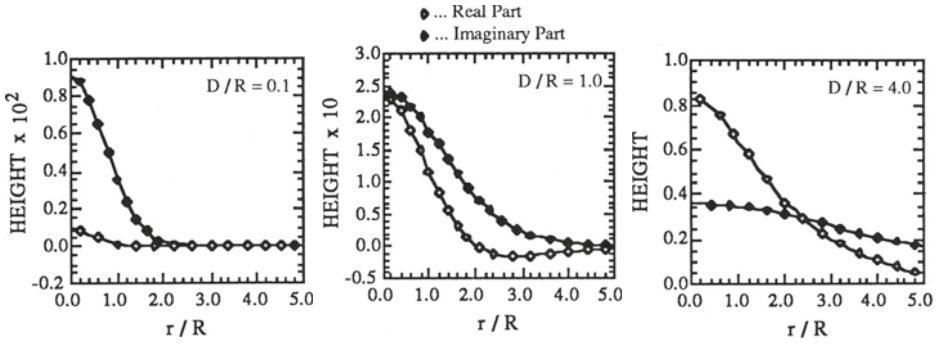

Fig. 2. Real and imaginary parts of the bump height for three different ratios of the diffusion length to the heating-beam radius. The abscissa is the radial distance from the center of the heating beam in units of the radius of that beam.

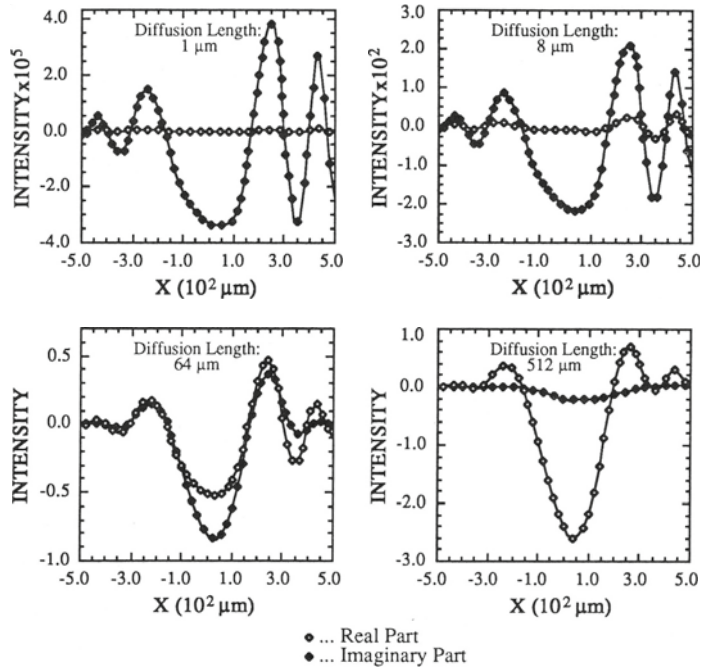

Fig. 3. Intensity distributions at a distance of 10 cm from the sample as a function of scan distance for 4 different values of the diffusion length with the heating and probe beams offset by a distance of 200 μm. The vertical scale is arbitrary but the relative scales from plot to plot are correct.

normal by an angle which may be as large a 40° or so. The calculation for a tilted beam is very similar to the one leading to Eq. (8), but the mathematical expressions involved in the derivation are significantly longer and will not be displayed here. Also, the experimental setup uses a line detector (a slit in front of a large-area detector) rather than the point detector assumed in calculating Figs. 1 and 3, and hence the signal corresponds to a line integral of Eq. (8) in the y-direction. Numerical calculations of these more complicated results are currently underway, but the computation time is greatly increased over that needed to evaluate Eq. (10), both by increase in the the number of parameters involved and by the destruction of the symmetry which allowed Eq. (8) to be reduced to Eq. (10). The results presented here are therefore to be considered as preliminary in the sense that they do not yet correspond to the exact experimental arrangement. However, it is expected that detailed curve fits of the more general formulae to the experimental data will allow the extraction of some of the thermal and elastic parameters of the sample from the data.

ACKNOWLEDGEMENT

This work was supported by the *Institute for Manufacturing Research*, Wayne State University.

REFERENCES

1. P.K. Kuo and M. Munidasa in *Review of Progress in Quantitative NDE,* Ed. D.O. Thompson and D.E. Chimenti, Vol **8** (to be published)
2. L.D. Favro, P.K. Kuo, and R.L. Thomas in *Review of Progress in Quantitative NDE,* Ed. D.O. Thompson and D.E. Chimenti, Vol **5A**, 439 (Plenum 1986)
3. L.D. Favro, S.M. Shepard, P.K. Kuo, and R.L. Thomas in *Review of Progress in Quantitative NDE,* Ed. D.O. Thompson and D.E. Chimenti, Vol **7A**, 225 (Plenum 1988)
4. L.D. Favro, S.M. Shepard, P.K. Kuo, and R.L. Thomas in *Photoacoustic and Photothermal Phenemona,* Ed. P. Hess and J. Pelzl, 370-380 (Springer-Verlag 1988)